Magnetic-Field Dependence of Direct Interband Tunneling in Germanium†

H. Roth,* W. Bernard,* and W. D. Straub*
Raytheon Research Division, Waltham, Massachusetts

and

J. E. Mulhern, Jr.
Department of Physics, University of New Hampshire, Durham, New Hampshire
(Received 9 August 1965; revised manuscript received 14 December 1965)

The effect of magnetic fields up to 110 kOe on the reverse current in Sb-doped germanium tunnel diodes has been investigated. A marked reduction in the tunnel current with magnetic field is observed at reverse biases greater than that corresponding to the onset of direct band-to-band tunneling, which occurs at the Kane voltage V_k. This effect is essentially temperature-independent from 1.8 to 300°K except for a thermal broadening in the vicinity of V_k, and assumes a maximum value with $\mathbf{H}\perp\mathbf{I}$. In addition, at low temperature and for $\mathbf{H}\|\mathbf{I}$, small oscillations with both magnetic field and bias are observed in the tunnel current. For $\mathbf{H}\|\mathbf{I}$, a theoretical treatment based on the formation of Landau levels yields good agreement with both the observed shift in the current-voltage characteristic and the oscillatory component. For $\mathbf{H}\perp\mathbf{I}$, a phenomenological treatment based on conventional tunneling theory and on the assumption of a magnetic-field-dependent Kane voltage is in good agreement with experiment. Analysis of the data yields a shift in V_k quadratic in the magnetic field, the constant of proportionality being $\sim 10^{-3}$ mV/kOe^2.

I. INTRODUCTION

Tunnel diodes have often been used to determine how the band structure of semiconductors is modified by such variables as pressure[1–3] and doping level.[4,5] It is well known that magnetic fields can also affect the band structure and transport properties of semiconducting materials. Esaki[6] was the first to observe small changes in the tunnel current in germanium diodes due to the presence of a magnetic field. Calawa *et al.*[7] observed a large magneto-tunneling effect in indium antimonide tunnel diodes and succeeded in intepreting the effect in terms of tunneling between Landau levels. They also confirmed Esaki's observations in the case of germanium. Oscillations in the tunnel current of indium antimonide diodes in an applied longitudinal magnetic field were reported by Chynoweth *et al.*[8]

It is the purpose of the present paper to investigate the effect of a magnetic field on the direct band-to-band tunnel current in germanium. Significant decreases in the reverse current were observed beyond the onset of direct tunneling. The effect was most striking in Sb-doped diodes, where indirect tunneling plays a minor role at low temperatures.

† Part of this work was performed at the National Magnet Laboratory which is supported at MIT by the U. S. Air Force Office of Scientific Research.

* Present address: National Aeronautics and Space Administration Electronics Research Center, Cambridge, Massachusetts.

[1] L. Esaki and Y. Miyahara, Solid-State Electron. **1**, 13 (1960).
[2] S. L. Miller, M. I. Nathan, and A. C. Smith, Phys. Rev. Letters **4**, 60 (1960).
[3] H. Fritzsche and J. J. Tiemann, Phys. Rev. **130**, 617 (1963).
[4] J. I. Pankove, Phys. Rev. Letters **4**, 20 (1960).
[5] W. Bernard, H. Roth, A. P. Schmid, and P. Zeldes, Phys. Rev. **131**, 627 (1963).
[6] L. Esaki (private communication).
[7] A. R. Calawa, R. H. Rediker, B. Lax, and A. L. McWhorter, Phys. Rev. Letters **5**, 55 (1960).
[8] A. G. Chynoweth, R. A. Logan, and P. A. Wolff, Phys. Rev. Letters **5**, 548 (1960).

In Sec. 2 we consider current-voltage characteristics in terms of Kane's theory of interband tunneling. This yields the various tunneling parameters, including the Kane voltage, required to treat the nonzero magnetic field case. In Sec. 3 we derive an expression for the direct tunnel current as a function of longitudinal magnetic field. The theory is shown to be in good agreement with the experimental results, including an observed oscillatory behavior. In Sec. 4 we present experimental results obtained with an applied transverse magnetic field. A magnetic-field-dependent Kane voltage forms the basis for a phenomenological treatment, which satisfactorily accounts for the experimental observations.

II. INTERBAND TUNNELING

Direct and indirect currents form the two essential contributions to the reverse characteristic of a germanium tunnel diode. These are illustrated in Fig. 1, which shows a schematic energy-band diagram for such a diode. Figure 1(a) shows the diode at low reverse bias. Indirect tunneling occurs between the [000] light-hole valence band maximum on the p side and the four [111] conduction band minima on the n side. Since tunneling takes place between two different points in k space, some additional process such as the absorption or emission of a phonon is required to conserve crystal momentum. When the reverse bias is increased such that the Fermi level on the p side is raised above the [000] conduction band minimum on the n side,

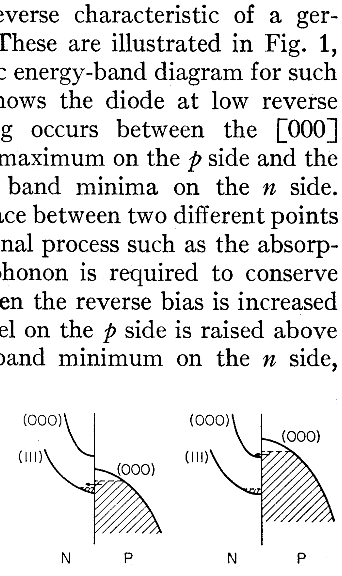

Fig. 1. Schematic energy-band diagram of a germanium tunnel diode showing (a) indirect tunneling at low reverse bias and (b) direct tunneling at a reverse bias $V > V_k$.

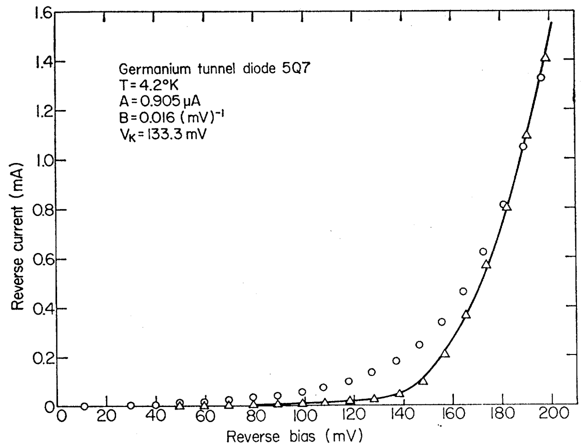

FIG. 2. Reverse current-voltage characteristic of a typical Sb-doped germanium tunnel diode at 4.2°K. The circles show the characteristic of the same diode at 300°K. The solid line shows the theoretical fit to the 4.2°K characteristic.

direct tunneling can occur. This is illustrated in Fig. 1(b). The voltage corresponding to the onset of direct tunneling is called the Kane voltage V_k.

We have carried out magneto-tunneling experiments on a number of reverse-biased germanium tunnel diodes. A series of diodes was fabricated with In-Ga-Zn dots alloyed on base material doped with from 4×10^{18} to 1×10^{19} antimony impurities cm^{-3}. Two crystal orientations of the base material were used, (100) and (111). The units were mounted in nonmagnetic microwave packages suitably modified to permit low-temperature operation.

Reverse current-voltage characteristics at 300 and 4.2°K are shown for a typical Sb-doped diode in Fig. 2. It should be noted that the characteristic at 4.2°K has a rather abrupt change in slope, designated as the Kane kink, which occurs when the reverse bias equals the Kane voltage.[9] The Kane kink is obscured in the 300°K characteristic by the large indirect current component. Since indirect tunneling requires phonons to conserve crystal momentum, the likelihood of such a process is greatly reduced at low temperatures by the reduced phonon population, thus leading to a more sharply defined onset of direct tunneling. It should be pointed out that the Kane kink is obscured even at low temperatures in As- and P-doped tunnel diodes, since these impurities can absorb the crystal momentum required for an indirect transition.

The reverse tunnel current in the absence of a magnetic field can be written as the sum of the indirect component I_i and the direct component I_d. We approximate the indirect current by

$$I_i=CV\exp(DV), \tag{1}$$

where the parameters C and D are evaluated from the low-bias current-voltage characteristic before the onset of direct tunneling.

An expression for the direct-tunneling component can be derived from Kane's theory of direct interband tunneling[10] by considering the potential diagram of a reverse-biased germanium junction as shown in Fig. 3. The tunneling transmission coefficient is

$$T=\frac{\pi^2}{9}\exp\left(-\frac{\pi m^{*1/2}\epsilon_g^{3/2}}{2e\hbar E}\right)\exp\left(-\frac{\epsilon_\perp}{\bar{\epsilon}_\perp}\right), \tag{2}$$

where ϵ_g is the direct band gap, $E=E_0(1+V/V_b)^{1/2}$ is the junction electric field, $m^*=m_cm_v/(m_c+m_v)$ is the reduced tunneling mass for the [000] conduction band of mass m_c and the light-hole valence band of mass m_v, and V_b is the junction built-in voltage, with $eV_b\simeq$the indirect band gap. In Eq. (2) the energy $\epsilon_\perp$ transverse to the direction of current flow is

$$\epsilon_\perp=\hbar^2k_\perp^2/2m^*, \tag{3}$$

where $k_\perp$ is the transverse wave vector, and

$$\bar{\epsilon}_\perp=e\hbar E/\pi m^{*1/2}\epsilon_g^{1/2}. \tag{4}$$

The current incident from the [000] conduction band in the elementary energy range $d\epsilon_{\perp c}d\epsilon_c$ is

$$dI_{\text{incident}}=(aem_c/2\pi^2\hbar^3)d\epsilon_{\perp c}d\epsilon_c, \tag{5}$$

where a is the junction area. Referring to Fig. 3, we see that the conservation of transverse wave vector $k_\perp$ requires that the limits on $\epsilon_{\perp c}$ for a given conduction band energy ϵ_c are 0 to either ϵ_c or $(m_v/m_c)\epsilon_v$, whichever is smaller. The transmitted direct current I_d is obtained by combining Eqs. (2) and (5), together with the

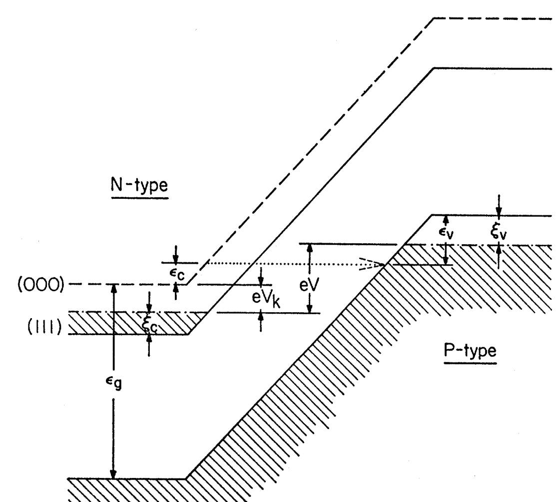

FIG. 3. Potential-energy diagram of a reverse-biased germanium tunnel diode, indicating the various energies referred to in the text. The dotted line represents a hole tunneling from the [000] conduction-band minimum to the (light-hole) valence band.

[9] J. V. Morgan and E. O. Kane, Phys. Rev. Letters 3, 466 (1959).

[10] E. O. Kane, J. Appl. Phys. 32, 83 (1961).

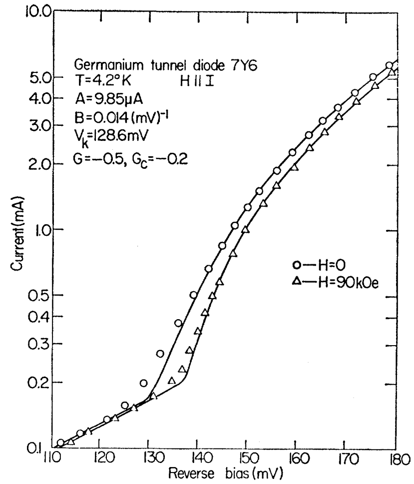

FIG. 4. Current-voltage characteristics of a reverse-biased Sb-doped germanium tunnel diode at 4.2°K with zero magnetic field and with an applied longitudinal field of 90 kOe. The solid curves are the characteristics predicted by the longitudinal theory derived in the text.

appropriate Fermi distributions, and integrating over ϵ_{1c} and ϵ_c. Near the onset of direct tunneling, where $e(V-V_k)<(m_v/m_c)\xi_v$, and at $T=0$°K this procedure yields

$$I_d=\frac{aem^*}{18\hbar^3}\bar{\epsilon}_\perp \exp\left(-\frac{\pi m^{*1/2}\epsilon_g{}^{3/2}}{2e\hbar E}\right)\times\left(e(V-V_k)-\frac{m^*}{m_c}\bar{\epsilon}_\perp\left\{1-\exp\left[-\frac{m_c e(V-V_k)}{m^*\bar{\epsilon}_\perp}\right]\right\}\right). \tag{6}$$

When the reverse bias is increased such that $e(V-V_k)>(m_v/m_c)\xi_v$, the expression for I_d becomes modified. However, Eq. (6) yields a good approximation for all $e(V-V_k)>0$ provided ξ_v is sufficiently $>\bar{\epsilon}_\perp$.

In order to compare Eq. (6) with experiment, we expand the weak voltage dependence in the tunneling exponent to first order in V and rewrite the expression in the approximate form

$$I_d\simeq A\gamma\exp(BV)\times\left((V-V_k)-\frac{0.15}{B}\gamma\left\{1-\exp\left[-\frac{B(V-V_k)}{0.15\gamma}\right]\right\}\right), \tag{7}$$

where

$$\gamma=(1+V/V_b)^{1/2}, \tag{8}$$

and

$$B=\pi m^{*1/2}\epsilon_g{}^{3/2}/4e\hbar V_b E_0, \tag{9}$$

E_0 being the zero-bias electric field in the junction. The parameters A, B, and the Kane voltage V_k are to be evaluated from experiment. We have taken $V_b=750$ mV [5] and $\epsilon_g=900$ mV,[11] and set $m_c=m_v=0.042m_0$.[12]

The solid line in Fig. 2 shows the fit to the experimental current-voltage characteristic at $T=4.2$°K achieved using Eqs. (1) and (7). The parameters A, B, and V_k were evaluated on an IBM 1620 computer using a method of successive approximations. Although V_k can be determined to better than $\pm 2\%$ by this procedure, the agreement of Eq. (7) with the zero-field characteristic is relatively insensitive to the values of A and B, provided they form a self-consistent set.

It is seen that the theoretical curve quite satisfactorily reproduces the experimental characteristic. For this diode the value of $V_k=133$ mV, and the calculated Fermi level on the n side is $\xi_c=17$ mV. This corresponds to an energy difference between the [000] and [111] conduction-band minima of 150±3 mV, in good agreement with the results of Zwerdling *et al.*[11] on pure germanium. Therefore it appears that, at least in this respect, the band structure remains essentially unchanged as the material is doped to degeneracy.

III. LONGITUDINAL MAGNETIC-FIELD DEPENDENCE OF DIRECT INTERBAND TUNNELING

The effect of a magnetic field parallel to the current on the tunneling characteristics of reverse-biased tunnel diodes was investigated using dc field intensities up to 110 kOe. The most striking result is that the entire reverse characteristic, including the Kane kink, is shifted to higher voltages by the magnetic field. This is illustrated in Fig. 4, which shows log$I$ versus V for a typical Sb-doped diode at 4.2°K with H equal to zero and 90 kOe. The diode was subjected to extensive electrolytic etching to assure a planar junction configuration, thus minimizing any contribution from the corresponding transverse field effect. The data presented in Fig. 4 are replotted in Fig. 5, which shows the relative

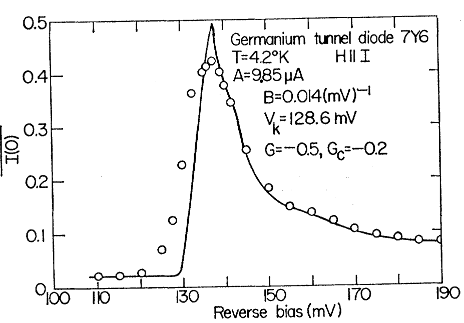

FIG. 5. Relative change of current due to a longitudinal magnetic field of 90 kOe as a function of reverse bias. The solid curve shows the theoretical fit to the data.

[11] S. Zwerdling, B. Lax, L. M. Roth, and K. J. Button, Phys. Rev. 114, 80 (1959).

[12] B. Lax and J. G. Mavroides, in *Solid State Physics*, edited by F. Seitz and D. Turnbull (Academic Press Inc., New York, 1960), Vol. 11, p. 390.

change in current $\Delta I(H)/I(O)$ as a function of the applied bias V. It is seen that $\Delta I(H)\ I(O)$ is small below V_k and increases sharply in the vicinity of V_k. In addition, evidence of an oscillatory behavior is observed in the bias region beyond the maximum.

Theories of tunneling in the presence of a longitudinal magnetic field have been derived by Haering and Adams[13] and by Argyres,[14] and the results have been used to interpret the magnetic-field dependence of direct interband tunneling in indium antimonide.[7] In order to discuss our experimental results for germanium, we shall derive an expression for the direct-tunnel current for arbitrary reverse bias $V \geq V_k$ under an applied longitudinal magnetic field. Although the zero-field notation of Kane[10] is retained, the approach is consistent with that adopted by Haering and Adams.[13]

A longitudinal magnetic field gives rise to cyclotron orbits quantized in a plane transverse to the direction of current flow. The magnetic quantum number n is conserved in a tunneling process. The "reduced" cyclotron energy $(n+\frac{1}{2})\hbar\omega^*$, together with the spin energy $\pm(g_c-g_v)\beta H$, constitutes the perpendicular energy $\epsilon_\perp$ [see Eq. (3)] for this case. Except for this distinction, tunneling proceeds exactly as in the zero-field case, so that the transmission coefficient of Eq. (2) is replaced by

$$T^{(\pm)}=\frac{\pi^2}{9}\exp\left(-\frac{\pi m^{*1/2}\epsilon_g^{3/2}}{2e\hbar E}\right)\times\exp\left\{-\frac{[n+\frac{1}{2}(1\pm G)]\hbar\omega^*}{\bar{\epsilon}_\perp}\right\}, \quad (10)$$

where the (+) and (−) signs refer to electrons having corresponding spin directions. The normalized g factors are given by

$$G=m^*\left(\frac{G_c}{m_c}-\frac{G_v}{m_v}\right),\quad G_c=\frac{m_c}{m_0}g_c,\quad G_v=\frac{m_v}{m_0}g_v. \quad (11)$$

For $m_c=m_v$, this reduces to

$$G=\tfrac{1}{2}(G_c-G_v). \quad (12)$$

We note that $T^{(\pm)}=0$ in Eq. (10) for $(V-V_k)<\frac{1}{2}(1\pm G_c)\hbar\omega_c$, since no direct tunneling can occur until the $n=0$ Landau level in the [000] conduction band falls below the Fermi level in the p-type material.

The elementary current incident from the [000] conduction band in the range $d\epsilon_c dk_\perp$ is found to be

$$dI^{(\pm)}{}_{\text{incident}}=[ae/(2\pi)^2\hbar]d\epsilon_c dk_\perp, \quad (13)$$

where $k_\perp$ now corresponds to the centers of the harmonic-oscillator wave functions along a transverse axis. We note that, for a given quantum number n and a given spin, conservation of perpendicular energy $\epsilon_\perp$ requires that the limits on ϵ_c are $[n+\frac{1}{2}(1\pm G_c)]\hbar\omega_c$ to either $e(V-V_k)$ or $\{e(V-V_k)+\xi_v-[n+\frac{1}{2}(1\mp G_v)]\hbar\omega_v\}$, whichever is smaller.

The transmitted direct current $I_d^{(\pm)}(H)$ in the presence of a longitudinal magnetic field is obtained by combining Eqs. (10) and (13), integrating over $k_\perp$ and ϵ_c, and summing over n. Assuming the bias voltage to be sufficiently low that $\xi_v \geq [n+\frac{1}{2}(1\mp G_v)]\hbar\omega_v$ for all Landau levels involved in the tunneling process, we find at $T=0°$K that

$$I_d^{(\pm)}(H)=\frac{ae}{36h}\exp\left(-\frac{\pi m^{*1/2}\epsilon_g^{3/2}}{2e\hbar E}\right)\times\sum_{n=0}^{N}\int_{[n+\frac{1}{2}(1\pm G_c)]\hbar\omega_c}^{e(V-V_k)}d\epsilon_c\int_{-eH/2\hbar}^{+eH/2\hbar}dk_\perp\times\exp\left\{-\frac{[n+\frac{1}{2}(1\pm G)]\hbar\omega^*}{\bar{\epsilon}_\perp}\right\}, \quad (14)$$

where N is the largest value of n for which

$$[n+\tfrac{1}{2}(1\pm G_c)\hbar\omega_c]\leq e(V-V_k).$$

Performing the indicated integrations over ϵ_c and $k_\perp$, this becomes

$$I_d^{(\pm)}(H)=\frac{aem^*}{36h^3}\hbar\omega^*\exp\left(-\frac{\pi m^{*1/2}\epsilon_g^{3/2}}{2e\hbar E}\right)\times\sum_{n=0}^{N}\{e(V-V_k)-[n+\tfrac{1}{2}(1\pm G_c)]\hbar\omega_c\}\times\exp\left\{-\frac{[n+\frac{1}{2}(1\pm G)]\hbar\omega^*}{\bar{\epsilon}_\perp}\right\}. \quad (15)$$

Finally, the summations over n can be performed by standard techniques to yield $I_d^{(\pm)}(H)$ in the form

$$I_d^{(\pm)}(H)=\frac{aem^*}{36h^3}\frac{\hbar\omega^*\exp(-\pi m^{*1/2}\epsilon_g^{3/2}/2e\hbar E)}{2\sinh(\hbar\omega^*/2\bar{\epsilon}_\perp)}\times\exp\left(\mp\frac{G\hbar\omega^*}{2\bar{\epsilon}_\perp}\right)\left(\left\{e(V-V_k)-\frac{m^*}{2m_c}(1\pm G_c)\hbar\omega^*\right\}-\left\{e(V-V_k)-[N+\tfrac{1}{2}(3\pm G_c)]\frac{m^*}{m_c}\hbar\omega^*\right\}\times\exp\left[-\frac{(N+1)\hbar\omega^*}{\bar{\epsilon}_\perp}\right]-\frac{m^*\hbar\omega^*\exp(-\hbar\omega^*/2\bar{\epsilon}_\perp)}{2m_c\sinh(\hbar\omega^*/2\bar{\epsilon}_\perp)}\times\left\{1-\exp\left[-\frac{(N+1)\hbar\omega^*}{\bar{\epsilon}_\perp}\right]\right\}\right). \quad (16)$$

[13] R. R. Haering and E. N. Adams, J. Phys. Chem. Solids **19**, 8 (1961).
[14] P. N. Argyres, Phys. Rev. **126**, 1386 (1962).

In the zero-field limit, where $(N+1)\hbar\omega_c \to e(V-V_k)$, this expression reduces to Eq. (6). We note that when the reverse bias is increased such that $[N+\frac{1}{2}(1\mp G_v)]\hbar\omega_v > \xi_v$, Eq. (16) for $I_d^{(\pm)}(H)$ becomes modified in a way analogous to the corresponding zero-field expression. Except for a small oscillatory component in $I_d^{(\pm)}(H)$, which we discuss below, Eq. (16) yields a good approximation for all $(V-V_k)>0$, provided ξ_v is sufficiently $>\bar{\epsilon}_\perp$. For convenience we rewrite Eq. (16) in terms of the zero-field parameters A and B [see Eqs. (6) and (7)] as

$$I_d^{(\pm)}(H) \simeq \frac{AB\exp(BV)\hbar\omega_c \exp(\mp GB\hbar\omega_c/0.3\gamma)}{0.6\sinh(B\hbar\omega_c/0.3\gamma)}\bigg(\{(V-V_k)-\tfrac{1}{2}(1\pm G_c)\hbar\omega_c\}-\{(V-V_k)-[N+\tfrac{1}{2}(3\pm G_c)\hbar\omega_c]\}$$
$$\times\exp\left[-\frac{(N+1)B\hbar\omega_c}{0.15\gamma}\right]-\frac{\hbar\omega_c\exp(-B\hbar\omega_c/0.3\gamma)}{2\sinh(B\hbar\omega_c/0.3\gamma)}\left\{1-\exp\left[\frac{(N+1)B\hbar\omega_c}{0.15\gamma}\right]\right\}\bigg). \quad (17)$$

The expression for $I_d^{(\pm)}(H)$ given by Eq. (17) represents a monotonically increasing function of V (or monotonically decreasing function of H) on which are superimposed small oscillations. The minima of the oscillations are determined by the condition

$$[N+\tfrac{1}{2}(3\pm G_c)]\hbar\omega_c=(V-V_k), \quad (18)$$

so that the period with respect to voltage at constant field is $\Delta V=\hbar\omega_c$, while the period with respect to reciprocal field at constant voltage is $\Delta(1/H)=\hbar/[m_c(V-V_k)]$. The envelope of the oscillatory minima, obtained from Eq. (17) by letting Eq. (18) be satisfied for all fields and voltages and adding the results for (+) and (−) spins, is

$$I_{d,\min}(H)=\frac{AB\exp(BV)\hbar\omega_c}{0.3\sinh(B\hbar\omega_c/0.3\gamma)}\left\{\left[(V-V_k)-\frac{\hbar\omega_c}{2}-\frac{\hbar\omega_c\exp(-B\hbar\omega_c/0.3\gamma)}{2\sinh(B\hbar\omega_c/0.3\gamma)}\right]\cosh\left(\frac{GB\hbar\omega_c}{0.3\gamma}\right)\right.$$
$$\left.+\frac{G_c\hbar\omega_c}{2}\sinh\left(\frac{GB\hbar\omega_c}{0.3\gamma}\right)+\frac{\hbar\omega_c\exp[-B(V-V_k)/0.15\gamma]}{2\sinh(B\hbar\omega_c/0.3\gamma)}\cosh\left[\frac{B(G-G_c)\hbar\omega_c}{0.3\gamma}\right]\right\}. \quad (19)$$

It is of interest to point out that, although no direct tunneling can occur until $(V-V_k)\geq\frac{1}{2}(1\pm G_c)\hbar\omega_c$, the expansion of Eq. (19) in powers of $\hbar\omega_c$ contains no linear term. Therefore, for small $\hbar\omega_c$, the over-all change in the tunneling current is quadratic in the magnetic field. The oscillatory component is given by

$$I_{d,\mathrm{osc}}(H)=\frac{AB\exp(BV)(\hbar\omega_c)^2\exp[-B(V-V_k)/0.15\gamma]}{1.2\sinh^2(B\hbar\omega_c/0.3\gamma)}\left\{\exp\left[-\frac{(G-G_c)B\hbar\omega_c}{0.3\gamma}\right]\right.$$
$$\times\left[\rho^{(+)}\exp\left(\frac{(1-\rho^{(+)})B\hbar\omega_c}{0.15\gamma}\right)+(1-\rho^{(+)})\exp\left(-\frac{\rho^{(+)}B\hbar\omega_c}{0.15\gamma}\right)-1\right]+\exp\left[+\frac{(G-G_c)B\hbar\omega_c}{0.3\gamma}\right]$$
$$\left.\times\left[\rho^{(-)}\exp\left(\frac{(1-\rho^{(-)})B\hbar\omega_c}{0.15\gamma}\right)+(1-\rho^{(-)})\exp\left(-\frac{\rho^{(-)}B\hbar\omega_c}{0.15\gamma}\right)-1\right]\right\}, \quad (20)$$

where

$$\rho^{(\pm)}=[N+\tfrac{1}{2}(3\pm G_c)]-(V-V_k)/\hbar\omega_c,\quad 0\leq\rho^{(\pm)}\leq1. \quad (21)$$

We note that the amplitude of the oscillations relative to $I_d(H)$ is attenuated by the factor $\exp[-B(V-V_k)/0.15\gamma]$ appearing in Eq. (20). Therefore the oscillations become more difficult to observe as the voltage is increased.

The solid curves in Figs. 4 and 5 represent theoretical fits to the data achieved using Eqs. (1), (7), and (17). The parameters A, B, and V_k were determined by fitting the current-voltage characteristic, as described previously, together with its magnetic field dependence. The parameter $C=C(H)$ appearing in Eq. (1) was modified to account for the weak magnetic-field dependence of the indirect-tunneling component. Normalized g factors, selected on the basis of the $\Delta I(H)/I(O)$ curve, were $G=-0.5$ and $G_c=-0.2$. According to Eq. (11) these correspond to a [000] conduction band g factor $g_c=-5$ and to a light-hole valence-band g factor $g_v=+20$.

The magnetic-field dependence of the direct tunnel current is shown in Fig. 6, where we have plotted $\Delta I_d(H)=I_d(O)-I_d(H)$ as a function of magnetic field for $V=165.8$ mV. The indicated bias voltage is sufficiently low for $\Delta I_d(H)$ to exhibit Landau-level oscillations of measurable amplitude, but high enough to permit observation of more than one complete period. We see that small oscillations in $\Delta I_d(H)$ can in fact be observed in Fig. 6. The oscillatory component alone

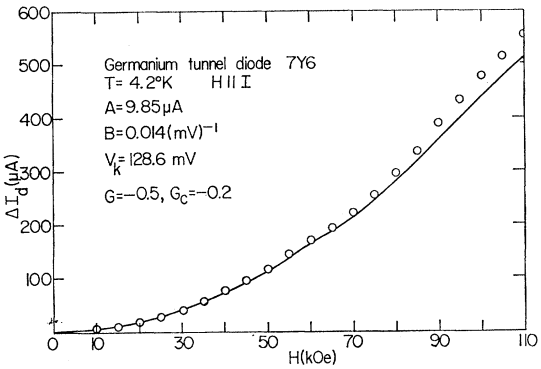

FIG. 6. Magnetic-field dependence of the change in direct tunnel current with $H \| I$ at a bias voltage $V=165.8$ mV. The solid curve represents the prediction of Eq. (17).

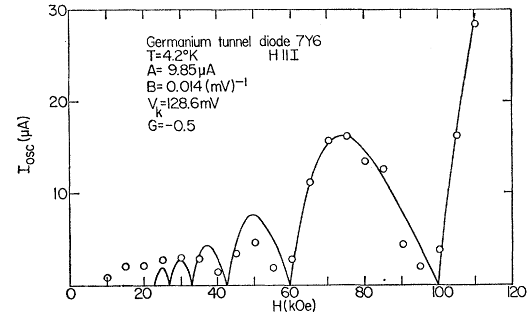

FIG. 7. The oscillatory component of the direct tunnel current as a function of magnetic field with $H \| I$ at a bias voltage $V=165.8$ mV. The solid curve represents the prediction of Eq. (22).

has been plotted as a function of H in Fig. 7 by expanding the current scale in Fig. 6 and subtracting $\Delta I_d(H)$ from the envelope of the maxima. The solid curve in Fig. 6 represents the prediction of Eqs. (17) and (7) using the parameters previously specified in fitting the current-voltage characteristics.

The oscillatory behavior should be described accurately by Eq. (20) for bias voltages such that $(V-V_k)<\xi_v$. For $(V-V_k)>\xi_v$ [see discussion following Eq. (16)] the oscillatory behavior becomes modified and additional structure appears. In the intermediate range where $(V-V_k)\sim\xi_v$ the situation becomes even more complex. Here the oscillations can alternate between the two types of behavior indicated above as the magnetic field is varied. Such a detailed analysis is not appropriate to the experimental results in their present form. However, we can illustrate the essential features of the oscillatory behavior by neglecting the relatively small spin splitting in the [000] conduction band. To accomplish this we set $G_c=0$ in Eq. (20), which results in the simplified expression

$$I_{d,\mathrm{osc}}(H)\simeq\frac{AB\exp(BV)(\hbar\omega_c)^2\exp[-B(V-V_k)/0.15\gamma]}{0.6\sinh^2(B\hbar\omega_c/0.3\gamma)}\times\cosh\frac{GB\hbar\omega_c}{0.3\gamma}\left\{\rho\exp\left[\frac{(1-\rho)B\hbar\omega_c}{0.15\gamma}\right]+(\rho-1)\exp\left[-\frac{\rho B\hbar\omega_c}{0.15\gamma}\right]-1\right\}, \quad (22)$$

where we note from Eq. (21) that $\rho^{(+)}=\rho^{(-)}=\rho$.

The solid curve in Fig. 7 shows the fit of Eq. (22) to the experimentally observed oscillations. It was found necessary to increase the effective mass $m^*=\frac{1}{2}m_{c,v}$ by $\sim 10\%$ in order to account for the magnetic field values at which the oscillatory minima occur.

IV. TRANSVERSE MAGNETIC-FIELD DEPENDENCE OF DIRECT INTERBAND TUNNELING

In the preceding section we have shown how the direct tunnel current depends on the magnetic field when H is parallel to the direction of current flow. As the angle between H and I is changed from 0 to 90°, $\Delta I(H)/I(O)$ increases by a factor ~ 2. For both crystal orientations used, no angular dependence of the effect is observed provided H remains in the junction plane.

The effect of a magnetic field transverse to the current on the reverse tunneling characteristics is shown in Fig. 8. As in the longitudinal case, the entire characteristic, including the Kane kink, is shifted to higher voltages by the magnetic field.

The only available discussion of tunneling in the presence of a transverse magnetic field appears to be that due to Haering and Adams.[13] The problem is quite difficult to treat theoretically, and the extension of the theory to the case of arbitrary bias voltage has not been carried out. However, the general implication of their

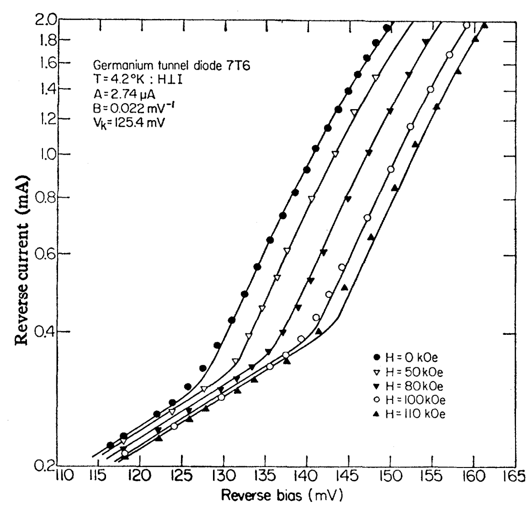

FIG. 8. Current-voltage characteristics of a reverse-biased Sb-doped germanium tunnel diode at $T=4.2$°K with applied transverse magnetic field as the parameter. The solid curves represent the phenomenological theory discussed in the text.

work is that a transverse field gives rise to an effective increase in the direct band gap quadratic in H. This would imply an attenuation of the tunneling exponential as well as a shift in the Kane voltage. However, we find that the experimental results can be accounted for by assuming that the Kane voltage alone is a function of the magnetic field. We therefore have modified Eq. (7) to read

$$I_d(H)=A\gamma\exp(BV)([V-V_k-\Delta V_k(H)]-(0.15\gamma/B)\times\{1-\exp[-B[V-V_k-\Delta V_k(H)]/0.15\gamma]\}), \quad (23)$$

where $\Delta V_k(H)$ denotes the shift in V_k with magnetic field.

The solid lines in Fig. 8 are the theoretical fits to the experimental data using Eqs. (1), (7), and (23) in conjunction with a least-squares determination of the shift in the Kane voltage. The magnetic field dependence of the Kane voltage is shown in Fig. 9, where we have plotted $\log\Delta V_k$ versus $\log H$. It is seen that ΔV_k exhibits a quadratic dependence on H,

$$\Delta V_k=\alpha H^2. \quad (24)$$

The constant of proportionality $\alpha=1.35\times10^{-3}$ mV/(kOe)^2 for this diode.

As in the longitudinal case, the onset of direct tunneling is clearly demonstrated by plotting the relative change in current $\Delta I(H)/I(O)$ as a function of applied bias. The sharp rise in the curve occurs at the Kane voltage, as is shown in Fig. 10 for diode 5Q7 using a magnetic field of 90 kOe. In contrast to the longitudinal results, no oscillatory behavior is evident. The effect shown is essentially temperature independent from 1.8 to 300°K except for a thermal broadening in the vicinity of V_k at elevated temperatures. It is of interest to note that the form of this curve is similar to that

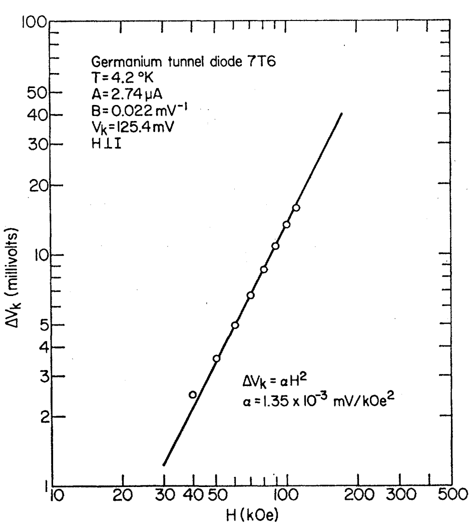

FIG. 9. Magnetic field dependence of ΔV_k with $H\perp I$.

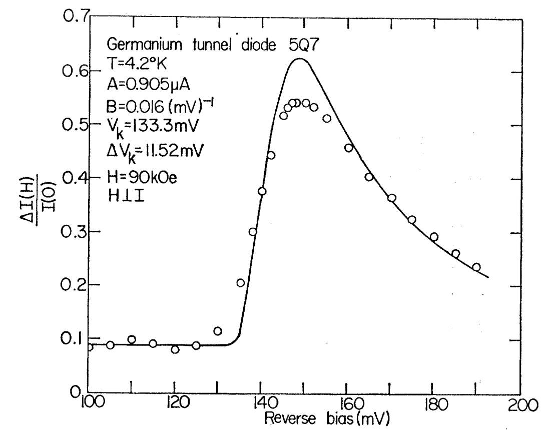

FIG. 10. Relative change of current due to a transverse magnetic field of 90 kOe as a function of reverse bias. The solid curve is obtained using the phenomenological treatment discussed in the text.

obtained by Fritzsche and Tiemann[3] in their study of the effects of elastic strain on interband tunneling in Sb-doped germanium. The solid curve of Fig. 10 represents the theoretical prediction of Eqs. (1), (7), and (23) using previously determined parameters obtained in connection with the zero-field fit to the I-V characteristic shown in Fig. 2.

The increase in V_k with magnetic field can be demonstrated in a striking way by considering the magnetic field dependence of the current in the immediate vicinity of the Kane kink. In this region the exponential in Eq. (23) for the direct current can be expanded so that, to lowest order in $[V-V_k-\Delta V_k(H)]$,

$$I_d(H)\simeq(AB/0.30)\exp(BV)[V-V_k-\Delta V_k(H)]^2. \quad (25)$$

Inserting Eq. (24) for the magnetic field dependence of V_k and subtracting the zero-field direct current, Eq. (25) can be written in the form

$$\begin{aligned}\Delta I_d(H)&=KH^2[2-\alpha H^2/(V-V_k)] \quad \text{for } (V-V_k-\alpha H^2)>0\\&=0 \quad \text{for } (V-V_k-\alpha H^2)<0,\end{aligned} \quad (26)$$

where K is assumed to be an arbitrary parameter implicitly dependent on the voltage.

In Fig. 11 we show $\log\Delta I_d$ versus $\log H$ at several bias voltages in the vicinity of V_k for diode 5Q7 with $H\perp I$. The change in the indirect current with magnetic field has been eliminated in accordance with Eq. (1). Also shown for comparison is ΔI_d at a reverse bias considerably in excess of V_k. Here ΔI_d is seen to exhibit a quadratic field dependence. However, for biases near V_k we see that, as H is increased, ΔI_d deviates monotonically from its quadratic field dependence until $\Delta V_k(H)=(V-V_k)$. At this point direct tunneling ceases, and no further decrease in the direct tunneling current can occur. The solid lines in Fig. 11 are theoretical fits to the data obtained by selecting appropriate

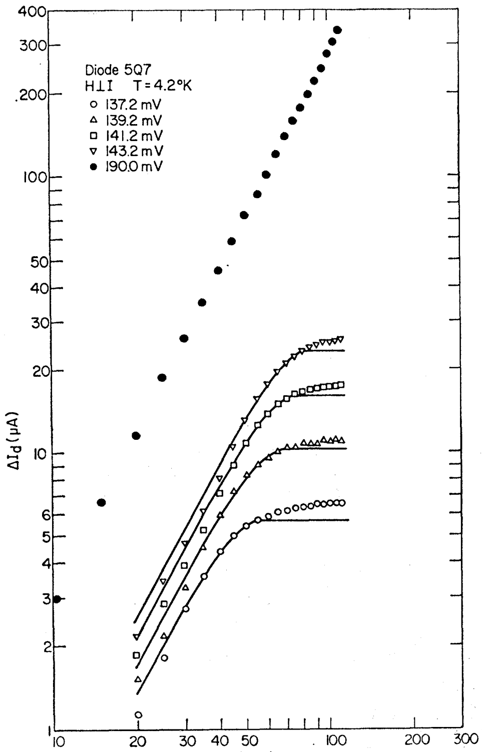

FIG. 11. Magnetic field dependence of the change in direct current at several bias voltages in the vicinity of V_k with $H \perp I$. Shown for comparison is the H dependence of ΔI at $V=190$ mV, which does not deviate from its quadratic behavior up to the highest fields studied. The solid lines are theoretical curves based on Eq. (26) in the text.

values of K and $\alpha/(V-V_k)$ in Eq. (26). We note that the cutoff of direct tunneling is less sharply defined than predicted by Eq. (26).

The Kane voltage V_k and the proportionality coefficient α in Eq. (24) are readily obtained by plotting $(V-V_k)/\alpha$ versus V, as shown in Fig. 12. We see that the experimental points, obtained from fitting Eq. (26) to the data of Fig. 11, exhibit the anticipated linear voltage dependence. The value of the Kane voltage obtained from Fig. 12 is $V_k=132.7$ mV, while $\alpha=1.36\times10^{-3}$ mV/(kOe)^2, in good agreement with the values $V_k=133.3$ mV and $\alpha=1.42\times10^{-3}$ mV/(kOe)^2 obtained from computer fits to the I-V characteristics for this diode.

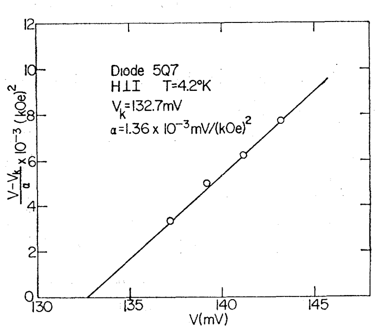

FIG. 12. Graphical determination of V_k and α from the data of Fig. 10.

V. SUMMARY

We have investigated the effect of a magnetic field on the direct interband tunneling current in reverse-biased germanium tunnel diodes. The application of a magnetic field results in a decrease in the current, a shift in the Kane voltage to higher values, and, for longitudinal fields, oscillations superimposed on the tunneling current as a function of both magnetic field and bias.

The effects in the case of a transverse magnetic field have been described phenomenologically by assuming a shift in the Kane voltage quadratic in H, with no corresponding attenuation of the tunneling exponential. The interpretation of this unexpected result must await a more comprehensive theoretical understanding of tunneling in a transverse magnetic field.

In the case of a longitudinal magnetic field a theoretical description based on the formation of Landau levels quantitatively accounts for the essential features of the experimental results including the oscillatory behavior. Preliminary g values for the [000] conduction band and the light-hole valence band were obtained which are in qualitative agreement with values appearing in the literature.[15,16]

Experiments are planned to investigate in greater detail the oscillatory behavior of the direct tunneling current under the influence of high longitudinal magnetic fields. It is anticipated that careful analysis of the structure appearing in the oscillations will yield useful information concerning the energy band parameters.

ACKNOWLEDGMENTS

We wish to thank the MIT National Magnet Laboratory for making the high magnetic field facilities available to us. We would like to express particular appreciation to L. J. Neuringer and L. G. Rubin for their interest and cooperation, and to P. Zeldes for his contribution to the early phases of the work. We would like to thank B. Wingerski for his advice on programming, and the University of New Hampshire Computation Center for the use of their facilities.

[15] J. M. Luttinger, Phys. Rev. **102**, 1030 (1956).
[16] L. M. Roth, B. Lax, and S. Zwerdling, Phys. Rev. **114**, 90 (1959).